

June 2001

Impact of the first SNO results on Neutrino Mass and Mixing

Abhijit Bandyopadhyay¹, Sandhya Choubey², Srubabati Goswami³, Kamales Kar⁴Saha Institute of Nuclear Physics,
1/AF, Bidhannagar, Calcutta 700 064, INDIA.

ABSTRACT

We investigate the implications of the SNO charged-current (CC) and electron scattering (ES) measurements of solar 8B neutrino fluxes for neutrino mass and mixing parameters by performing a global and unified χ^2 analysis of the solar neutrino data in the framework of two neutrino mixing. We consider both $\nu_e - \nu_{active}$ and $\nu_e - \nu_{sterile}$ solutions and perform (i) analysis of the total rates data of Cl, Ga, SK and SNO experiments and (ii) global analysis including the total rates data, the recoil electron spectrum data of SK and the CC spectrum observed at SNO. For the $\nu_e - \nu_{active}$ case the inclusion of the SNO results in the analysis of the total rates reduces (enhances) the goodness-of-fit (GOF) of the SMA(LMA) solution. The flat spectrum observed at SK further favours the LMA solution over the SMA solution and no allowed area is obtained in the SMA region at 3σ level from the global analysis. For the $\nu_e - \nu_{sterile}$ case, with the inclusion of the SNO results, all the solutions are disfavoured with a probability of more than 99% from the total rates analysis while for the global analysis the GOF of these become much worse.

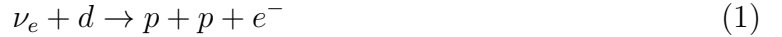
¹ abhi@theory.saha.ernet.in

² sandhya@theory.saha.ernet.in

³ sruba@theory.saha.ernet.in, currently at Physical Research Laboratory, Ahmedabad, India

⁴ kamales@tnp.saha.ernet.in

The Sudbury Neutrino Observatory (SNO) has declared its first results [1] on the measurement of solar 8B neutrinos through the CC detection process



in the heavy water (D_2O) of SNO. This reaction is sensitive to only ν_e and the observed ν_e flux is

$$\Phi_{CC}^{SNO} = 1.75 \pm 0.07(stat)_{-0.11}^{+0.12}(sys) \times 10^6 cm^{-2} s^{-1}$$

whereas the expectation from the standard solar model (SSM) of [2] is $5.05 \times 10^6 cm^{-2} s^{-1}$. SNO also gives the 8B flux measured by the electron scattering (ES) reaction



as

$$\Phi_{ES}^{SNO} = 2.39 \pm 0.34(stat)_{-0.14}^{+0.16}(sys) \times 10^6 cm^{-2} s^{-1}$$

The reaction (2) is sensitive to both ν_e and ν_μ or ν_τ and the measured flux is in agreement with that observed by the SuperKamiokande (SK) detector [3, 4] via the same reaction

$$\Phi_{ES}^{SK} = 2.32 \pm 0.03(stat)_{-0.07}^{+0.08} \times 10^6 cm^{-2} s^{-1}$$

These new generation high statistics experiments thus confirm the solar neutrino deficit observed in the pioneering Cl experiment [5] and subsequently in Kamiokande [6] and the low threshold Ga experiments SAGE, GALLEX and GNO [7]. A comparison of the 8B ν_e flux measured by the CC reaction (1) with the flux of 8B neutrinos measured at SK signifies the presence of a ν_μ and/or ν_τ component in the solar neutrino flux at 3.3σ level. The total 8B neutrino flux derived from a comparison of Φ_{CC}^{SNO} and the SK observed flux Φ_{ES}^{SK} is found to be $5.44 \pm 0.99 \times 10^6 cm^{-2} s^{-1}$ which is in excellent agreement with the SSM predictions [2].

In Table 1 we show the latest results for the total rates measured in Cl [5], Ga [7], SK (1258 days) [4] and SNO (CC and ES) experiments with respect to (w.r.t) the SSM fluxes of BPB00 [2]. The numbers in the parentheses for SK and SNO (ES) are when the ν_μ or ν_τ contributions are subtracted. We also show the composition of the major fluxes in each of these experiments. For the Ga rates we give the weighted average of SAGE, GALLEX and GNO. Apart from the total rates SNO also gives the CC spectrum of the 8B neutrinos and they do not report any significant distortion with energy. SK has published the data on the recoil electron energy spectrum in separate day and night bins and also the zenith angle distribution of events [8, 9]. They do not find any significant variation of the data with energy and although there

is a slight excess of the number of events observed in the night-time when the neutrinos are passing through the earth's matter, the effect is only at 1.3σ .

Various particle physics solutions assuming non standard neutrino properties have been considered to account for the deficit [10, 11]. The simplest possibility is two flavor neutrino oscillation which requires ν_e to mix with some other flavor of neutrino. But even in this scenario there are several disconnected allowed regions in the mass-squared difference - mixing angle parameter space consistent with the global solar neutrino data. The flat recoil electron energy spectrum observed at SK has been responsible in creating a vast change in the allowed oscillation regions and their goodness of fit (GOF) as compared to those obtained from analysis of total rates only [12] -[19]. The best-fit to the data on total rates in Cl, Ga and Kamiokande and/or SuperKamiokande experiments was coming in the MSW [20] Small-Mixing-Angle (SMA) region. But with the flat electron energy spectrum observed in SK the best-fit in the global analysis of rates and spectrum data shifted to the Large-Mixing-Angle (LMA) region. The fit in the LOW region (low $\Delta m^2 \sim 10^{-7} \text{ eV}^2 - 10^{-8} \text{ eV}^2$), where earth matter effect regenerates the low energy neutrinos also became good. From the total rates data vacuum oscillation (VO) of neutrinos were allowed with best-fit $\Delta m^2 \sim 8.5 \times 10^{-11} \text{ eV}^2$. But in the global analysis with the SK electron spectrum data this became largely disfavoured as the energy dependence of the survival probability in this region picked up conflict with the flat electron recoil energy spectrum. Recent analysis by SK [21] and other groups [17, 19] do find good fits in vacuum oscillation region for $\Delta m^2 \sim 4 - 5 \times 10^{-10} \text{ eV}^2$ where the energy averaging over the bins smears out the energy dependence of the probability and the flat spectrum observed in SK can be accounted for. However the allowed regions are very tiny around the Δm^2 values in the vacuum oscillation region as well as somewhat fragile depending on the method of data fitting followed [17] unlike the MSW allowed regions which are quite robust against these changes. Apart from these pure MSW and pure vacuum regions, a grey zone ($\Delta m^2 \sim 5 \times 10^{-10} \text{ eV}^2 - 10^{-9} \text{ eV}^2$) called the Quasi-Vacuum-Oscillation (QVO) regime is allowed. For this area of the parameter space both matter effects inside the sun and the effects due to coherent oscillation phases are important. Thus there is a continuity in the allowed parameter regions and the older practice of separate analysis of the data in vacuum and MSW regions were replaced by what is called unified analysis which uses a general expression for probability valid in the whole mass range $10^{-12} - 10^{-3} \text{ eV}^2$. The cutoff in the Δm^2 from above is due to the constraint from the CHOOZ reactor experiment [22]. Another new aspect was the appearance of the dark zones ($\theta > \pi/4$) [23]. In the background of this picture emerging out from detailed analysis of the available solar neutrino data several studies had been made on the expectations and implications of the SNO results [17],[24] -[27]. Now work has started to find the allowed values of mass squared differences and mixing parameters by actually incorporating the SNO results in the oscillation analysis [28, 29, 30].

In this paper we investigate the significance of the SNO results for neutrino mass

and mixing parameters by including these in the χ^2 -analysis of the global solar neutrino data on total rates in Cl, Ga and SK experiments and the SK day-night recoil electron spectrum. The definition of χ^2 used by us is,

$$\chi^2 = \sum_{i,j} (F_i^{th} - F_i^{exp}) (\sigma_{ij}^{-2}) (F_j^{th} - F_j^{exp}) \quad (3)$$

where i,j runs over the experimental data points. Here $F_i^\alpha = \frac{T_i^\alpha}{T_i^{BPB00}}$ where α is *th* (for the theoretical prediction) or *exp* (for the experimental value) and T_i is the total rate in the i th experiment. We first do an analysis with the total rates given in Table 1. The error matrix σ_{ij} contains the experimental errors, the theoretical errors and their correlations. For evaluating the error matrix for the total rates case we use the procedure described in [31]. The details of the code used by us can be found in [11, 15, 16]. For the rate of $\nu_e - d$ CC events recorded in the SNO detector we use

$$R_{CC} = \frac{\int dE_\nu \lambda_{\nu_e}(E_\nu) \sigma_{CC}(E_\nu) \langle P_{ee} \rangle}{\int dE_\nu \lambda_{\nu_e}(E_\nu) \sigma_{CC}(E_\nu)} \quad (4)$$

$$\sigma_{CC} = \int_{E_{Ath}} dE_A \int_0^\infty dE_T R(E_A, E_T) \frac{d\sigma_{\nu_e d}(E_T, E_\nu)}{dE_T} \quad (5)$$

where λ_{ν_e} is the normalized 8B neutrino spectrum, $\langle P_{ee} \rangle$ is the time averaged ν_e survival probability, $d\sigma_{\nu_e d}/dE_T$ is the differential cross section of the $\nu_e - d$ interaction, E_T is the true and E_A the apparent(measured) total energy of the recoil electrons, E_{Ath} is the detector threshold energy which we take as $(6.75+m_e)$ MeV, where m_e is the rest mass of the electron and $R(E_A, E_T)$ is the energy resolution function for which we use the expression in [1]. One of the major uncertainties in the SNO CC measurement stems from the uncertainty in the $\nu_e - d$ cross-section. We use the cross-sections from [32] which are in agreement with [33]. Both calculations give an uncertainty of 3% which is also the value quoted in [1]⁵.

The expression for ν_e survival probability according to an unified formalism over the mass range $10^{-12} - 10^{-3}$ eV² and for the mixing angle θ in the range $[0, \pi/2]$ is well documented [35, 36, 23] and can be expressed as

$$P_{ee} = P_\odot P_\oplus + (1 - P_\odot)(1 - P_\oplus) + 2\sqrt{P_\odot(1 - P_\odot)P_\oplus(1 - P_\oplus)} \cos \xi \quad (6)$$

where P_\odot denotes the probability of conversion of ν_e to one of the mass eigenstates in the sun and P_\oplus gives the conversion probability of the mass eigenstate back to the ν_e

⁵It was recently pointed out in [34] that the calculation of both [32] and [33] underestimate the total $\nu_e - d$ cross-section by 6%. We have not included this effect in our calculation.

state in the earth. All the phases involved in the Sun, vacuum and inside Earth are included in ξ . This most general expression reduces to the well known MSW (the phase ξ is large and averages out) and vacuum oscillation limit (matter effects are absent and the phase ξ is important) for appropriate values of $\Delta m^2/E$. The procedure which we use for calculating P_{\oplus} and P_{\odot} in MSW, vacuum as well as the in-between quasi-vacuum (QVO) regions where both ξ and matter effects are relevant is discussed in [19].

The results for the analysis of total rates for $\nu_e - \nu_{active}$ oscillations are presented in Table 2 for both pre-SNO and post-SNO cases. As far as the pre-SNO total rates are concerned both SMA and vacuum oscillation give good fits with the best-fit coming in the SMA region. For post-SNO the best-fit comes in the VO region. However the noticeable thing is that with the inclusion of the SNO data the GOF of both SMA and VO becomes worse and that in the LMA region becomes better. Prior to SNO, at the best-fit point obtained in the SMA region, the observed Cl and Ga rates were described very well but the predicted SK rate was higher. With the introduction of SNO CC rate, the best-fit shifts towards higher Δm^2 and higher $\tan^2 \theta$, which corresponds to a lower survival probability for the 8B neutrinos thus lowering the SK and SNO rate. But this also lowers the Cl rate and the over all χ^2 becomes high.

In the LMA region the survival probabilities of the high energy neutrinos are given as [37]

$$P_{ee}^{LMA} \approx \frac{1}{2}(1 - \epsilon) + f_{reg} \quad (7)$$

where $\epsilon = \cos 2\theta$ and $f_{reg} = P_{2e} - \sin^2 \theta$, P_{2e} being the probability of $\nu_2 \rightarrow \nu_e$ conversion inside the Earth. Since the observations of three of the experiments (Cl, SK and SNO) which are mainly sensitive to 8B neutrinos are now close, they can be well described through a single eq. (7) and the GOF of the LMA solution becomes better. For low energies relevant for Ga the matter effects are weak and

$$P_{ee}^{LMA} \approx \frac{1}{2}(1 + \epsilon^2) \quad (8)$$

which gives a greater probability as compared to eq.(7) for the same ϵ and the Ga rate of Table 1 is accounted for. There is no significant improvement for the LOW solution for which the probability is given by eq. (8) for all energies. In Table 2 we also give the GOF of the Just So² solution [38]. In this region one gets a very small survival probability for the 7Be neutrinos while for the 8B neutrinos the survival probability is close to 1.0 [39]. Since this scenario does not give any suppression of the 8B flux it gets disfavoured with a probability of more than 99% by our total rates analysis with the 8B flux normalization fixed at the BPB00 SSM value. We have also displayed in Table 2 the results of the χ^2 analysis including the SNO ES rate in addition to the SNO CC rate. The inclusion of the SNO ES rate in the analysis improves the overall quality of the fits for all the solutions but it still has large statistical error and does not make any significant difference between the relative fit of various solutions.

In Figs. 1 and 2 we plot the allowed regions for pre-SNO and post-SNO (excluding ES scattering) respectively at 90% ($\chi^2 \leq \chi_{min}^2 + 4.61$), 95% ($\chi^2 \leq \chi_{min}^2 + 5.99$), 99% ($\chi^2 \leq \chi_{min}^2 + 9.21$) and 99.73% C.L. ($\chi^2 \leq \chi_{min}^2 + 11.83$) from an analysis of total rates. Since the GOF of the SMA solution becomes worse with the inclusion of the SNO CC rate the SMA region reduces in size in Fig. 2. Also it shifts towards higher values of $\tan^2 \theta$. On the other hand the allowed area in the LMA region becomes slightly bigger in the post-SNO case as the GOF in the LMA region improves. In the LOW region we get allowed areas at 95% C.L. for the post-SNO case.

In Table 3 we present the best-fit values of parameters, χ_{min}^2 and the GOF of the solutions for the $\nu_e - \nu_{sterile}$ solution from an analysis of total rates. The GOF in the SMA region goes down from 16.04% (pre-SNO) to 0.03% after including the SNO CC rate. Since the observed SNO CC rate is significantly lower than the observed ES rate at SK, pure $\nu_e - \nu_{sterile}$ transitions are highly disfavoured and this is responsible for the bad fit obtained in Table 3 after including the SNO results.

For the global analysis the total χ^2 is defined as

$$\chi^2 = \chi_{rates}^2 + \chi_{skspec}^2 + \chi_{snospec}^2 \quad (9)$$

where χ_{skspec}^2 and $\chi_{snospec}^2$ are the χ^2 for the SK recoil electron spectrum and SNO CC spectrum respectively and χ_{rates}^2 corresponds to the χ^2 from the total rates data. For the calculation of the rates part i,j runs from 1 to 4 if we do not include the ES rate measured in SNO and 1 to 5 if we include the ES rate from SNO; for the SK spectrum part i,j runs from 1 to 38 corresponding to 19 day and 19 night bins; for the SNO CC spectrum i,j runs from 1 to 11. To account for the fact the ES rate measured in SK is not independent of the spectrum we vary the normalization of the spectrum as a free parameter. Similarly for SNO CC spectrum we introduce a free normalization to avoid overcounting with the total CC rate. For the calculation of the error matrix for the SK spectrum we include the statistical error, correlated and uncorrelated systematic errors and the error due to the calculation of the spectrum [8, 21]. For the SNO CC spectrum we include the statistical error and the correlated systematic errors from [1]. For all our analyses presented in this paper we keep the 8B flux normalization fixed at SSM value.

The no-oscillation $\chi^2/d.o.f$ is 100.31/52 which is disfavored at 99.99% C.L. from the global data. In Table 4 we show the results of global analysis of the rates and the spectrum data for oscillation to an active flavour. To highlight the impact of the SNO data we present the results for cases with and without SNO⁶. For both pre-SNO and post-SNO we give the best-fit points and the local χ_{min}^2 in five regions – SMA, LMA, LOW-QVO, VO and Just So².

The pre-SNO analysis indicates that with the inclusion of the SK day-night spectrum data the GOF of the SMA solution becomes worse and fit in the LMA and LOW

⁶ The pre-SNO best-fit values for the global analysis are from [19]. The corresponding C.L. contours also appear in [19].

regions become much better, with LMA giving the best-fit. This worsening of fit in the SMA region is owing to the fact that the peculiar energy dependence of the observed rates in Cl, Ga and SK experiments favour larger values of $\tan^2 \theta$ while the flat recoil electron energy spectrum observed by SK prefers smaller values of $\tan^2 \theta$. LMA and LOW solutions on the other hand can describe the flat recoil electron spectrum at SK very well and the GOF in these regions are much better. For the VO case, with the inclusion of the SK spectrum data the best-fit shifts to $\Delta m^2 \sim 4.55 \times 10^{-10} eV^2$ for which energy averaging gives an approximately constant probability for the high energy neutrinos. The Just So² solution, although disfavoured from the rates analysis at more 99% C.L., can explain the flat SK spectrum well and thus gets allowed from the global analysis at 17.14%.

With the inclusion of the SNO CC rate into the global analysis, the data on total rates demand still higher values of $\tan^2 \theta$ for the SMA solution, thus enhancing the conflict between the rates and SK spectrum data and the GOF becomes worse in the SMA region⁷. If we look at the post-SNO χ_{min}^2 in Table 4 for the case excluding the SNO CC spectrum and the ES data then we find that the SMA solution becomes more disfavoured with SNO, while LMA, LOW and VO are seen to improve, with the best-fit still in the LMA region. The Just So² solution gets worse with the introduction of the SNO CC rate, however it is still allowed with a probability of 8.1%.

We have repeated the post-SNO global analysis by including the SNO ES rate and the SNO CC spectrum in addition to the SNO CC rate and have presented the results in Table 4. We find that due to large errors, both statistical and systematic, the effect of addition of the SNO CC spectrum in the analysis is to increase the $\chi^2/d.o.f$ and hence reduce the GOF for all the solutions in general.

In Fig. 3 we show the allowed regions at 90%, 95%, 99% and 99.73% C.L. obtained from the global analysis for $\nu_e - \nu_{active}$ transitions including *all published SNO data*. The significant change in the allowed regions after including the SNO results is the disappearance of the SMA region even at 99.73% C.L. (3σ) as a result of increased conflict between the total rates and SK spectrum data. For the Just So² solution also there is no allowed region at 99.73% C.L. after including the SNO data in the global analysis of rates and SK spectrum⁸.

In Table 5 we present the results of global analysis for $\nu_e - \nu_{sterile}$ solution and as expected the fits become worse with the inclusion of SNO results. The SMA and the VO solutions which were allowed at 22.9% and 32.57% respectively without the SNO results are now allowed at only 5.12% and 6.10%. The GOF in the LMA and LOW regions also become worse. Prior to the SNO results the SMA and VO was giving much better fit to the global data as compared to the LMA and LOW solutions since

⁷The contribution from χ_{rates}^2 to the total χ^2 increases from 6.39 at the SMA best-fit for the pre-sno case to 14.99 with the inclusion of the SNO CC rate reducing the overall GOF.

⁸From Table 4 we see that for the pre-SNO case we have allowed area at 99.73% C.L. in the Just So² region.

the former could account for the total rates data much better. But with the inclusion of the SNO CC rate the GOF of the SMA and VO solutions for the total rates analysis is reduced by a large amount and as a result all the solutions become more disfavoured for the sterile neutrino case.

The GOF of the SMA solution is very sensitive to the uncertainty of the $\nu_e - d$ cross-sections used. To illustrate this point in Table 6 we give the GOF of the various solutions for the $\nu_e - \nu_{active}$ case using the $\nu_e - d$ cross-sections from [40] and a conservative estimate of uncertainty of 9%. Comparing the GOF in the LMA and SMA region from the global analysis we find that with the use of a 9% uncertainty in the $\nu_e - d$ cross-sections the SMA region gets allowed at the 3σ level.

To summarise, we include the recent SNO results in global χ^2 analysis of the solar neutrino data assuming ν_e to mix with either another active neutrino or a sterile neutrino. We first perform a fit to the total rates including (i) the SNO CC rate and (ii) both SNO CC and SNO ES rates, along with the total rates from Cl, Ga and SK experiments. For the $\nu_e - \nu_{active}$ case, SMA, LMA, LOW and VO solutions which were allowed from pre-SNO total rates analysis are still allowed but the inclusion of the SNO CC data in the analysis of *total rates* worsens the GOF of the SMA and VO solution and betters the GOF of the LMA solution. The inclusion of the SNO CC rate disfavours all the solutions for pure $\nu_e - \nu_{sterile}$ case with a probability of more than 99%.

We next perform a global analysis of rates and spectrum data including (i) the SNO CC rate and (ii) the SNO CC and ES rates and the SNO CC spectrum along with the total rates of Cl, Ga and SK experiments and the SK day-night spectrum. For $\nu_e - \nu_{active}$ case, the global analysis gives five allowed solutions – LMA, VO, LOW, SMA, Just So² – in order of decreasing GOF. However no allowed area is obtained at 99.73% C.L. for SMA and Just So² solutions. With the inclusion of the SNO CC rate the mismatch between the best-fit parameters for the rates and SK spectrum increases in the SMA region while the LMA gives a very good fit to the global data. This results in a marked improvement of the LMA solutions over the SMA solution and we get no allowed area in the SMA region even at the 3σ level.

The sterile neutrino alternative gets highly disfavoured by the rates analysis and the global analysis gives a GOF of only about 5% in the SMA region. However for an arbitrary 8B flux normalization, a small admixture with the sterile neutrino state cannot be ruled out completely as is shown by the model-independent analysis performed in [41].

Note added: Our paper (hep-ph/0106264) appeared on the net at about the same time as [28] and [29]. We have updated our calculation with the latest $\nu_e - d$ cross-sections from [32]. Our method of analysis is same as in [28] but we have included transitions to sterile neutrinos not included in [28]. For the active case our results agree with [28]. The analysis in [29] uses a somewhat different definition of χ^2 and they include an extra parameter to determine the active-sterile admixture in their

analysis. We have also presented results including the SNO ES rate and the SNO CC spectrum data in our analysis, not included in the analyses of [28] and [29].

The authors would like to thank D.P. Roy for his valuable comments and suggestions. S.G. would like to thank the theory group of Physical Research Laboratory for their hospitality.

References

- [1] Q.R. Ahmad *et al.*, <http://www.sno.phy.queennsu.ca/sno/firstresults/>, nucl-ex/0106015.
- [2] J.N. Bahcall, S. Basu, M. Pinsonneault, *Ap. J.* **555**, 990 (2001).
- [3] Y. Fukuda *et al.* (The Super-Kamiokande collaboration), *Phys. Rev. Lett.* **81**, 1158 (1998); erratum **81**, 4279 (1998).
- [4] Y. Fukuda *et al.*, *Phys. Rev. Lett.* **86**, 5651 (2001).
- [5] B.T. Cleveland *et al.* *Astrophys. J* **496**, 505 (1998).
- [6] Y. Fukuda *et al.*, (The Kamiokande collaboration), *Phys. Rev. Lett.* **77**, 1683 (1996).
- [7] J.N. Abdurashitov *et al.*, (The SAGE collaboration), *Phys. Rev. Lett.* **77**, 4708 (1996); *Phys. Rev. C* **60**, 055801 (1999); W. Hampel *et al.*, (The Gallex collaboration), *Phys. Lett.* **B388**, 384 (1996); *Phys. Lett.* bf B447, 127 (1999); Talk presented in Neutrino 2000 held at Sudbury, Canada (T.A. Kirsten for The Gallex collaboration), *Nucl. Phys. B Proc. Suppl.* **77**, 26 (2000); M. Altmann *et al.*, (The GNO collaboration), *Phys. Lett.* bf B492,16 (2000); Talk presented in Neutrino 2000 held at Sudbury, Canada (E. Bellotti for the GNO Collaboration) *Nucl. Phys. B Proc. Suppl.* **91** 44 (2001).
- [8] Y. Fukuda *et al.* (The Super-Kamiokande collaboration), *Phys. Rev. Lett.* **82**, 2430 (1999).
- [9] Y. Fukuda *et al.* (The Super-Kamiokande collaboration), *Phys. Rev. Lett.* **82**, 1810 (1999).
- [10] S. Choubey, S. Goswami, D. Majumdar, *Phys. Lett.* **B484**, 73 (2000). O.G. Miranda, C. Peña-Garay, T.I. Rashba, V.B. Semikoz, J.W.F. Valle, *Nucl. Phys.* **B595**, 360 (2001); D. Majumdar, A. Raychaudhuri and A. Sil, *Phys. Rev.* **D63**, 073014 (2001); A.M. Gago, H. Nunokawa and R. Zukanovich Funchal, *Nucl. Phys. Proc.*

- Suppl. **100**, 68 (2001); M.M. Guzzo, H. Nunokawa, P.C. de Holanda, O.L.G. Peres, hep-ph/0012089; J. Pulido, hep-ph/0106201.
- [11] A. Bandyopadhyay, S. Choubey, S. Goswami, Phys. Rev. **D63**, 113019 (2001).
 - [12] J.N. Bahcall, P.I. Krastev and A.Yu. Smirnov, Phys. Rev. **D58**, 096016 (1998).
 - [13] M.C.Gonzalez-Garcia and C. Peña-Garay, Nucl. Phys. Proc. Suppl. **91**, 80 (2000); M.C. Gonzalez-Garcia, P.C. de Holanda, C. Peña-Garay, and J.W.F. Valle, Nucl. Phys. **B573**, 3 (2000).
 - [14] V. Barger and K. Whisnant, Phys. Lett. **B456**, 54 (1999).
 - [15] S. Goswami, D. Majumdar and A. Raychaudhuri, hep-ph/9909453.
 - [16] S. Goswami, D. Majumdar and A. Raychaudhuri, Phys. Rev. **D63**, 013003 (2001).
 - [17] J.N. Bahcall, P.I. Krastev, and A.Yu. Smirnov, JHEP **0105**, 015 (2001).
 - [18] S. Choubey, S. Goswami, N. Gupta and D.P. Roy, hep-ph/0103318, to appear in Phys. Rev. **D**.
 - [19] S. Choubey, S. Goswami, K. Kar, A.R. Antia, S.M. Chitre, hep-ph/0106168.
 - [20] L. Wolfenstein, Phys. Rev. **D34**, 969 (1986); S.P. Mikheyev and A.Yu. Smirnov, Sov. J. Nucl. Phys. **42(6)**, 913 (1985); Nuovo Cimento **9c**, 17 (1986) .
 - [21] Y.Fukuda *et al.* Phys. Rev. Lett. **86**, 5656 (2001).
 - [22] M. Apollonio et al., Phys. Lett. **B446**, 415 (1999).
 - [23] A.de. Gouvea, A. Friedland, H. Murayama, Phys.Lett.**B490**, 125, (2000).
 - [24] J. N. Bahcall , P.I. Krastev , A. Yu. Smirnov JHEP **0105**, 015 (2001).
 - [25] J.N. Bahcall , P. I. Krastev, A. Yu. Smirnov Phys. Rev. **D63**, 053012 (2001).
 - [26] J. N. Bahcall, P.I. Krastev , A. Yu. Smirnov, Phys. Rev. **D62**, 093004, (2000).
 - [27] V. Barger, D. Marfatia, K. Whisnant and B.P. Wood, hep-ph/0104095.
 - [28] G.L. Fogli, E. Lisi, D. Montanino and A. Palazzo, hep-ph/0106247.
 - [29] J.N. Bahcall, M.C. Gonzalez-Garcia and C. Penya-Garay, hep-ph/0106258.
 - [30] P. Creminelli, G. Signorelli, A. Strumia, hep-ph/0102234 (updated version, july 2000).

- [31] G.L. Fogli and E. Lisi, *Astropart. Phys.* **3**, 185 (1995).
- [32] S. Nakamura, T. Sato, V. Gudkov and K. Kubodera, *Phys. Rev.* **C63**, 034617 (2001).
- [33] M. Butler, J. Chen and X. Kong, *Phys. Rev.* **C63**, 034617, (2001).
- [34] J.F. Beacom and S.J. Parke, hep-ph/0106128.
- [35] S.T. Petcov, *Phys. Lett.* **B214**, 139, (1988); **200**,373, (1988); S.T. Petcov and J. Rich, *Phys. Lett.* **B426**, (1989).
- [36] G.L. Fogli, E. Lisi, D. Montanino, A. Palazzo , *Phys. Rev.* **D62**, 113004, (2000).
- [37] M.C. Gonzalez-Garcia, C. Peña-Garay, Y. Nir and A. Yu. Smirnov, *Phys. Rev.* **D63**, 013007 (2001).
- [38] R.S. Raghavan, *Science* **267**, 45 (1995); P.I. Krastev and S.T. Petcov, *Phys. Rev.* **D53**, 1665 (1996).
- [39] See Fig. 5 of [17].
- [40] <http://www.sns.ias.edu/~jnb/>, J.N. bahcall and E. Lisi *Phys. Rev.* **D54**, 5417 (1996).
- [41] V. Barger, D. Marfatia and K. Whisnant, hep-ph/0106207.

Table 1: The ratio of the observed solar neutrino rates to the corresponding BPB00 SSM predictions used in this analysis.

experiment	$\frac{obsvd}{BPB00}$	composition
Cl	0.335 ± 0.029	B (75%), Be (15%)
Ga	0.584 ± 0.039	pp (55%), Be (25%), B (10%)
SK	0.459 ± 0.017 (0.351 ± 0.017)	B (100%)
SNO(CC)	0.347 ± 0.027	B (100%)
SNO(ES)	0.473 ± 0.074 (0.368 ± 0.074)	B (100%)

Table 2: The best-fit values of the parameters, χ_{min}^2 , and the goodness of fit from an analysis of the total rates given in Table 1 for $\nu_e - \nu_{active}$.

	Nature of Solution	Δm^2 in eV^2	$\tan^2 \theta$	χ_{min}^2	Goodness of fit
pre-SNO (Cl+Ga+SK)	SMA	5.96×10^{-6}	1.39×10^{-3}	0.30	58.39%
	LMA	2.40×10^{-5}	0.31	2.91	8.80%
	LOW-QVO	1.34×10^{-7}	0.64	7.49	0.62%
	VO	8.79×10^{-11}	0.43	0.32	57.16%
	Just So ²	5.40×10^{-12}	1.00	12.86	$3.36 \times 10^{-2}\%$
post-SNO (Cl+Ga+SK + SNO CC)	SMA	7.71×10^{-6}	1.44×10^{-3}	5.44	6.59%
	LMA	2.59×10^{-5}	0.34	3.40	18.27%
	LOW-QVO	1.46×10^{-7}	0.67	8.34	1.55%
	VO	7.73×10^{-11}	0.27	2.49	28.79%
	Just So ²	5.38×10^{-12}	1.29	19.26	$6.57 \times 10^{-3}\%$
post-SNO (Cl+Ga+SK +SNOCC +SNOES)	SMA	7.71×10^{-6}	1.44×10^{-3}	5.44	14.23%
	LMA	2.32×10^{-5}	0.33	3.47	32.47%
	LOW-QVO	1.14×10^{-7}	0.81	9.24	2.63%
	VO	7.74×10^{-11}	0.27	2.92	40.41%
	Just So ²	5.38×10^{-12}	1.27	19.42	$2.24 \times 10^{-2}\%$

Table 3: The best-fit values of the parameters, χ_{min}^2 , and the goodness of fit from an analysis of the total rates given in Table 1 for $\nu_e - \nu_{sterile}$.

	Nature of Solution	Δm^2 in eV ²	$\tan^2 \theta$	χ_{min}^2	Goodness of fit
pre-SNO (Cl+Ga+SK)	SMA	4.43×10^{-6}	1.44×10^{-3}	1.97	16.04%
	LMA	6.41×10^{-5}	0.58	17.45	$2.94 \times 10^{-3}\%$
	LOW-QVO	1.49×10^{-7}	0.85	18.01	$2.19 \times 10^{-3}\%$
	VO	8.99×10^{-11}	0.36	2.70	10.03%
	Just So ²	5.40×10^{-12}	1.00	12.89	$3.30 \times 10^{-2}\%$
post-SNO (Cl+Ga+SK +SNOCC)	SMA	4.18×10^{-6}	5.72×10^{-4}	17.24	$1.80 \times 10^{-2} \%$
	LMA	4.98×10^{-5}	0.54	23.96	$6.27 \times 10^{-4}\%$
	LOW-QVO	1.00×10^{-7}	0.94	24.26	$5.40 \times 10^{-4}\%$
	VO	1.07×10^{-10}	0.27	15.71	$3.88 \times 10^{-2}\%$
	Just So ²	5.37×10^{-12}	1.28	19.40	$6.13 \times 10^{-3}\%$
post-SNO (Cl+Ga+SK + SNO CC + SNO ES)	SMA	5.20×10^{-6}	4.38×10^{-4}	17.34	$6.02 \times 10^{-2} \%$
	LMA	6.61×10^{-5}	0.55	24.42	$2.04 \times 10^{-3}\%$
	LOW-QVO	2.96×10^{-8}	0.87	22.16	$6.04 \times 10^{-3}\%$
	VO	7.86×10^{-11}	0.23	23.76	$2.80 \times 10^{-3}\%$
	Just So ²	5.37×10^{-12}	1.27	19.56	$2.09 \times 10^{-2}\%$

Table 4: The best-fit values of the parameters, χ_{min}^2 , and the goodness of fit from the global analysis of rate and spectrum data for $\nu_e - \nu_{active}$.

	Nature of Solution	Δm^2 in eV ²	$\tan^2 \theta$	χ_{min}^2	Goodness of fit
pre-SNO (Cl+Ga+SK + SK spec)	SMA	5.48×10^{-6}	4.88×10^{-4}	43.59	24.57%
	LMA	5.08×10^{-5}	0.35	34.73	62.14%
	LOW-QVO	1.55×10^{-7}	0.66	38.50	44.66%
	VO	4.55×10^{-10}	0.44	37.80	47.86%
	Just So ²	5.43×10^{-12}	1.00	46.13	17.14%
post-SNO (Cl+Ga+SK +SNOCC +SK spec)	SMA	5.28×10^{-6}	3.75×10^{-4}	51.14	9.22%
	LMA	4.70×10^{-5}	0.38	33.42	72.18%
	LOW-QVO	1.76×10^{-7}	0.67	39.00	46.99%
	VO	4.64×10^{-10}	0.57	38.28	50.25%
	Just So ²	5.37×10^{-12}	0.77	51.90	8.10%
post-SNO (all data)	SMA	5.29×10^{-6}	3.89×10^{-4}	65.20	7.30%
	LMA	4.49×10^{-5}	0.38	47.84	56.05%
	LOW-QVO	1.70×10^{-7}	0.66	53.30	34.85%
	VO	4.53×10^{-10}	0.36	56.82	23.60%
	Just So ²	5.37×10^{-12}	0.78	66.29	6.12%

Table 5: The best-fit values of the parameters, χ_{min}^2 , and the goodness of fit from the global analysis of rates and spectrum data for $\nu_e - \nu_{sterile}$.

	Nature of Solution	Δm^2 in eV ²	$\tan^2 \theta$	χ_{min}^2	Goodness of fit
pre-SNO	SMA	4.03×10^{-6}	4.9×10^{-4}	44.11	22.90%
	LMA	6.09×10^{-5}	0.56	47.15	14.67%
	LOW-QVO	3.08×10^{-8}	0.85	47.16	14.65%
	VO	4.54×10^{-10}	0.39	41.37	32.57%
	Just So ²	5.39×10^{-12}	1.00	45.61	18.51%
post-SNO (all data)	SMA	3.87×10^{-6}	3.69×10^{-4}	67.37	5.12%
	LMA	7.66×10^{-5}	0.48	67.37	5.12%
	LOW-QVO	2.89×10^{-8}	1.00	68.19	4.45%
	VO	4.67×10^{-10}	0.30	66.31	6.10%
	Just So ²	5.37×10^{-12}	0.78	66.48	5.93%

Table 6: The best-fit values of the parameters, χ^2_{min} , and the goodness of fit using $\nu_e - d$ cross section from [40].

	Nature of Solution	Δm^2 in eV ²	$\tan^2 \theta$	χ^2_{min}	Goodness of fit
post-SNO (Cl+Ga+SK +SNOCC)	SMA	6.13×10^{-6}	1.46×10^{-3}	2.97	22.65%
	LMA	2.30×10^{-5}	0.32	3.26	19.59%
	LOW-QVO	1.40×10^{-7}	0.70	7.88	1.93%
	VO	7.95×10^{-11}	0.27	2.20	33.29%
	Just So ²	5.37×10^{-12}	0.92	14.25	$8.05 \times 10^{-2}\%$
post-SNO (Cl+Ga+SK +SNOCC +SK spec)	SMA	5.36×10^{-6}	4.15×10^{-4}	45.21	22.85%
	LMA	4.45×10^{-5}	0.36	34.98	65.38%
	LOW-QVO	1.56×10^{-7}	0.69	38.38	49.80%
	VO	4.54×10^{-10}	2.35	37.83	52.31%
	Just So ²	5.37×10^{-12}	0.88	46.93	17.94%

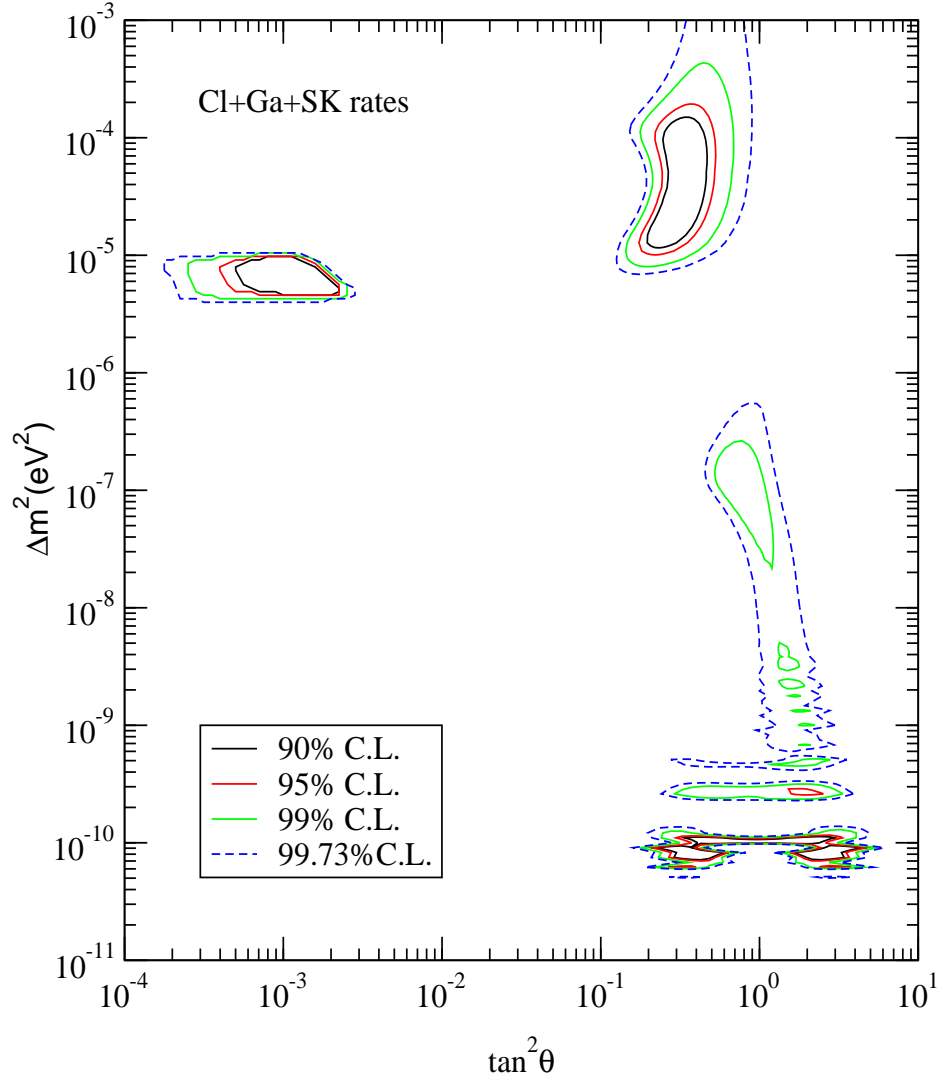


Figure 1: The pre-SNO 90%, 95%, 99% and 99.73% C.L. allowed area from the fit to the data on total rates from the Cl, Ga and SK experiments assuming two-generation oscillations to active neutrino.

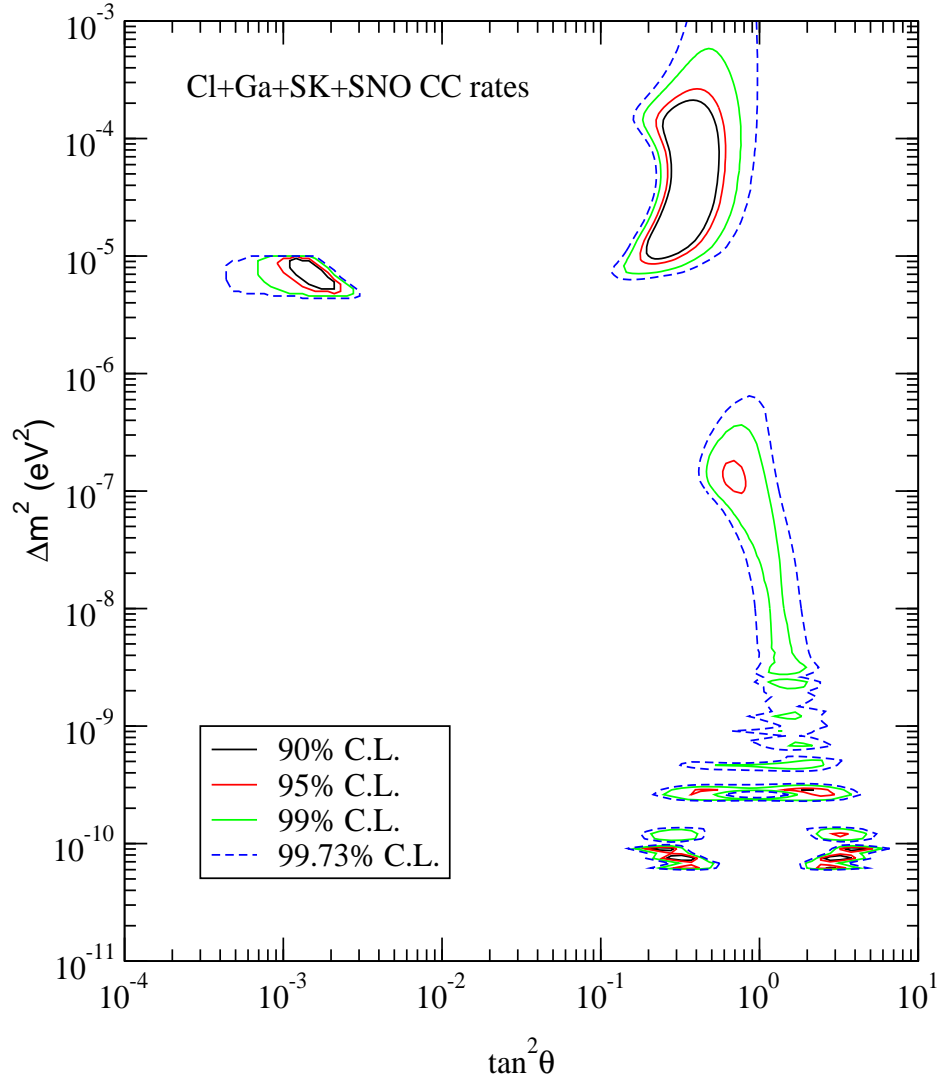


Figure 2: The post-SNO 90%, 95%, 99% and 99.73% C.L. allowed area from the fit to the data including the SNO CC rate along with the total rates from the Cl, Ga, SK experiments for two-generation oscillations to active neutrino.

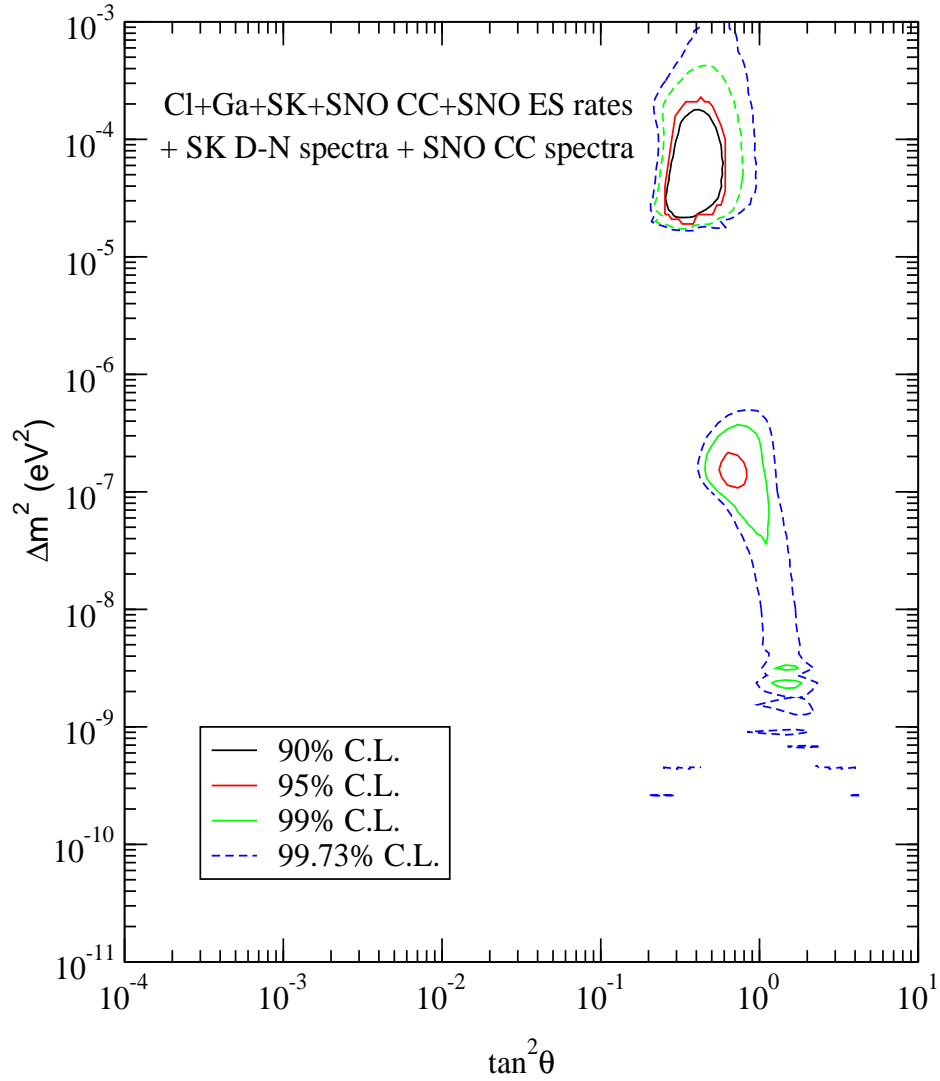


Figure 3: The post-SNO 90%, 95%, 99% 99.73% C.L. allowed area from the global analysis of the total rates from Cl, Ga, SK and SNO (both CC and ES), the 1258 day SK recoil electron energy spectrum at day and night and the SNO CC spectrum data, assuming two-generation oscillations to active neutrino.